

# Nonlinear Finite Element Analysis of Plain Concrete Members Subjected to Torsion

David A.M.Jawad

University of Basrah / Engineering College, Basrah, Iraq

Mohammed M.Handhal\*

University of Basrah / Engineering College, Basrah, Iraq

\* Qbcivil@yahoo.com

This work aims at studying the behavior of rectangular-section plain concrete beams subjected to torsion by using the finite element method. A theoretical study is presented on sixty one beam specimens divided into four series. Series one, includes twelve plain normal strength concrete (NSC) specimens, and the main parameters in the series are the compressive strength of concrete and the section dimensions. In series two, the same parameters are investigated for fifteen plain high strength concrete (HSC) specimens.

The results show that the size of the beams is found to be the most important parameter that affects ultimate torque in the plain concrete beams, and that the torsional capacity increases in direct proportion to section dimensions. for NSC and HSC beams respectively. The failure in the plain concrete beams is sudden.

A comparison with elastic, plastic and skew bending theories is conducted for the plain concrete beams, and a good estimate for torsional strength value can be achieved for small size beams by using the plastic theory, whereas the elastic theory underestimates the torsional strength when compared with the other theories.

Maximum values of 113% and 460% are calculated for the increase in torsional capacity for NSC and HSC beams respectively.

## 1. General

A moment acting about the longitudinal axis of a member is called a **twisting moment**, a **torque**, or a **torsional moment**,  $T$ .

## 2. Behavior Of Plain Concrete Members Subjected To Pure Torsion

A plain concrete member subjected to pure torsion will crack and fail along 45° spiral lines because of the diagonal tension corresponding to the torsional stresses [2]. Fig. (1-5), The shear stress on the section distributes consistently with that obtained from the elastic analysis at the early loading stage, and the maximum shear stress appears at the center of the longer edge (mid-depth). In addition, the maximum principal tensile stress is equal to the maximum shear stress and occurs at the same point but with an inclination of 45°, because the shear stresses exist in pairs and the normal stress is neglected [4].

The shear stress of the member increases with the torsion acting, and the plastic strain of concrete occurs slightly. When the maximum principal tensile stress of the concrete reaches the tensile strength, the inclined crack appears first on the middle of the side surface (longer edge of the section) and is perpendicular to the principal tensile stress. Afterwards, the inclined crack extends both upwards and downwards along the inclination of about 45° and then turns on the top and bottom surfaces (short edges of the section). After the three surfaces are cracked, the member is torn in two

pieces along the fourth surface (longer edge of the section) with a twist failure surface Fig. (1-5), but no crack is usually found on the other place. Generally, the ultimate torsion is

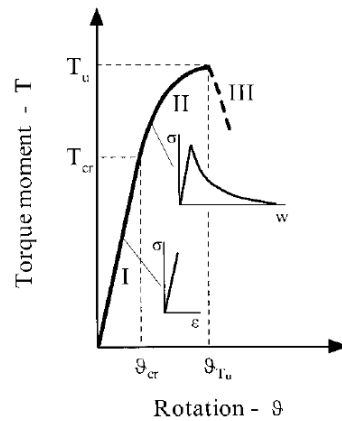


**Figure (1-5) Member of plain concrete under pure torsion [4]**

slightly greater, but by no more than 10%, than the cracking torsion of the member, as shown in Fig. (1-6) [4].

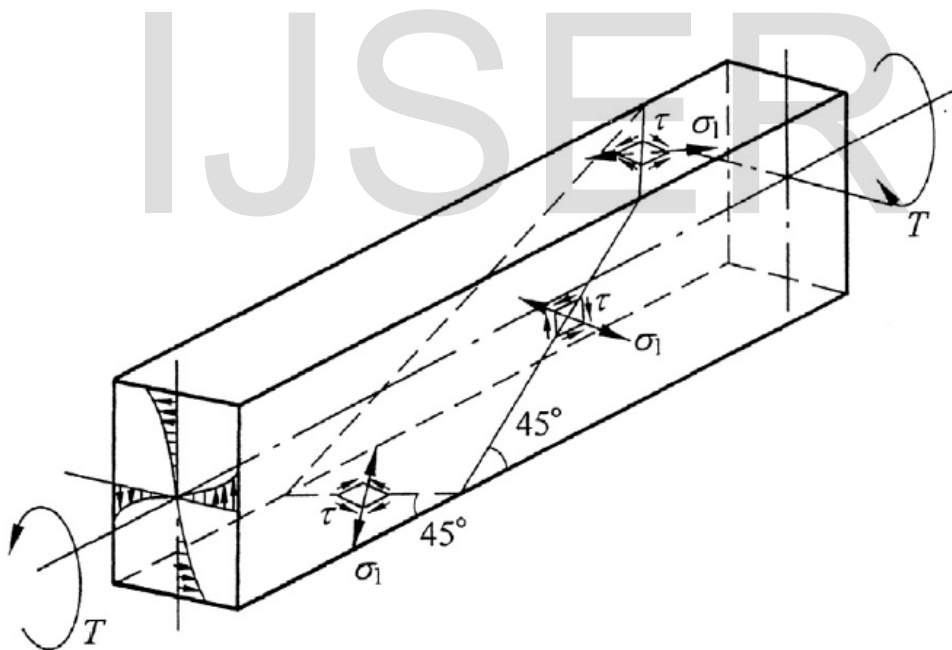


**Figure (1-6) Behavior of Plain Concrete Element in Pure Torsion[3]**

### 3. Torsion of Plain Concrete Members

Three theories have been developed to predict the torsional strength of plain concrete members. These are elastic theory, plastic theory, and skew bending theory.

### 3.1 Elastic theory

The behavior of a torsional member is reasonably well described by St. Venant's theory as the theory also extended to the prediction of torsional strength. The elastic theory assumed that the concrete is a homogeneous material and stresses are distributed according to Saint-Venant's theory. [6].

$$T_e = \alpha x^2 y f_t \quad (1.2)$$

where; ( $T_e$ ) is the elastic torsional resistance for plain concrete rectangular beam, ( $\alpha$ ) is a function of ( $y/x$ ), ( $y$ ) is the longer side of the section, and ( $x$ ) is the shorter side of the section.

### 3.2 Plastic theory

Tests have shown that the elastic theory consistently underestimates the failure strength of a plain concrete beam, the actual test strength is roughly 50% greater than that predicted by the elastic theory. To achieve better accuracy plastic theory is often applied to concrete based on Nadai's sand heap analogy. The torsional resistance is then given as twice the volume confined by the surface, and concrete assumed to have infinite plasticity.  $T_p$  can therefore be expressed by

$$T_p = \alpha_p x^2 y f_t \quad (1.5)$$

( $\alpha_p$ ) is the plastic coefficient, it varies from 0.333 to 0.5.

$$\alpha_p = \frac{1}{2} - \frac{x}{6y} \quad (1.6)$$

### 3.3 Skew bending theory

$$T_u = \frac{b^2 \cdot h}{3} (0.85 f_r) \quad (1.13)$$

## 4. Details of Study

The structural behavior of a cantilever rectangular-section plain concrete beams is simulated within the context of the finite element method using the ANSYS code. Two series of plain concrete beams based on experimental works (Hsu [7], Bakhsh et. al. [80]) were

investigated, and the major variables that characterized the beams include concrete strength, and size of the beams.

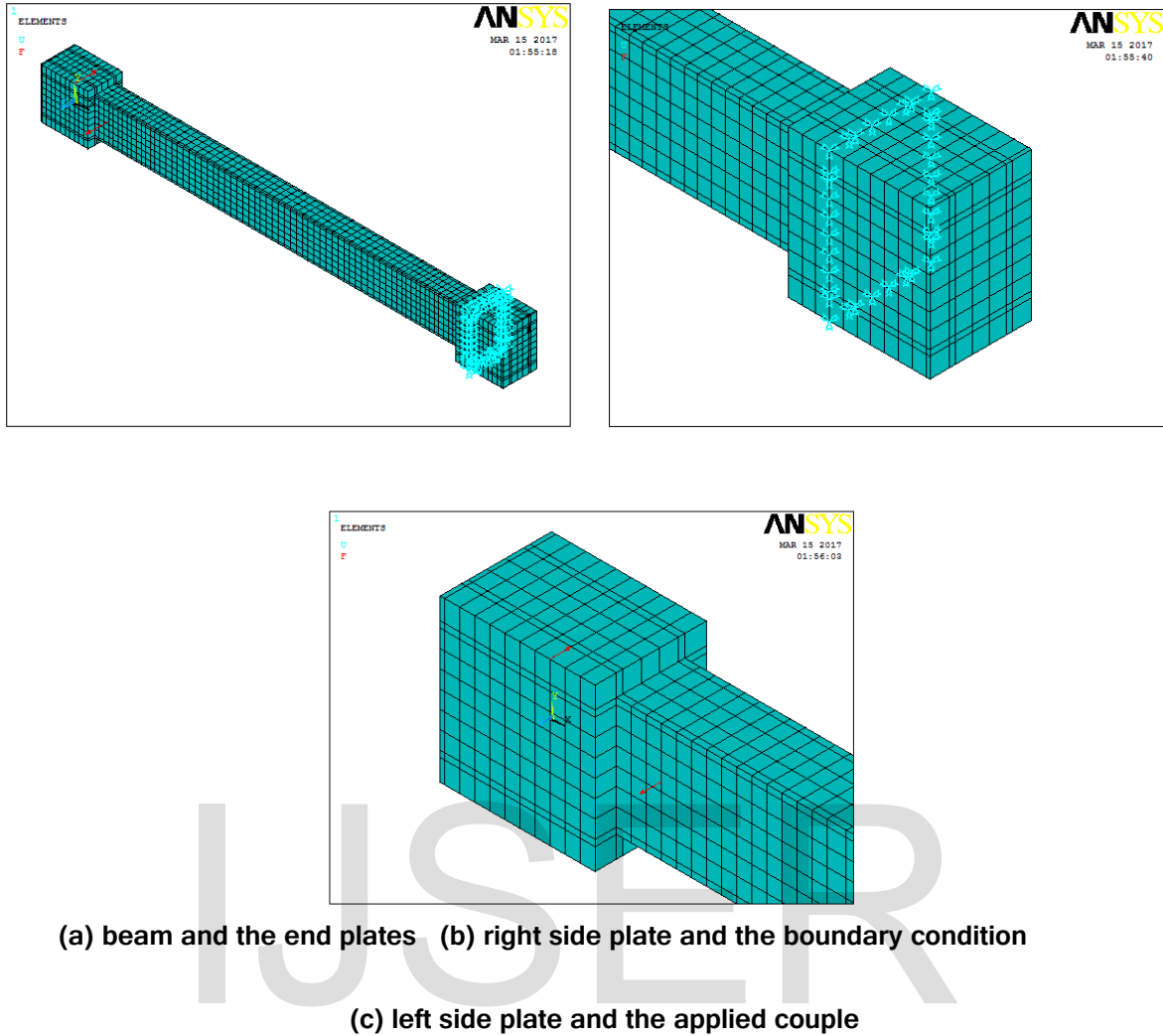
## 5. Finite element modeling

### 5.1 Load and Boundary Conditions

It is important to apply the boundary conditions to get a solution, it is obvious that each set of boundary conditions will lead to a unique solution, since the displacement boundary conditions are required to constrain the model. To ensure that the specimens are modeled correctly, boundary conditions must be applied at the right places where the supports and loadings exist in the experimental test.

The support was modeled as a closed steel box comprising plates that surround the concrete beam end, these plates are fixed at the right end of the beam. The line of nodes on the plates along the x, y and z-direction were constrained.

The torsion on the beam was applied as a couple on the steel plate at the left side. Fig. (4-1) illustrates the steel plates and applied couple and boundary conditions.



(a) beam and the end plates (b) right side plate and the boundary condition  
(c) left side plate and the applied couple

Figure (4-1): Load and boundary conditions

## 5.2 The Model Geometry and Materials Properties

The plain concrete beams, surrounding end plates, and supports are modeled by creating nodes first on the working plane of ANSYS 14. Then the elements are created through nodes with auto-numbering of elements, this method is helpful to control the mesh size and number of the elements of the model.

The Solid 65 element is used to represent the concrete. Link 180 elements are used to create the longitudinal and transverse reinforcement. The element type number, material number,

and real constant set number for the ANSYS models are set for each mesh. At the right-hand end of the beam, the displacement in all directions is held at zero, and referred to as a fixed support.

The ANSYS program provides us with several options to characterize different types of material behavior, such as bilinear isotropic (with work hardening) and multi-linear isotropic hardening. The concrete is assumed to behave as a homogeneous and initially isotropic material. The multilinear isotropic representation for compressive uniaxial stress-strain relationship are used for concrete model. For reinforcement steel, the bilinear isotropic representation is assumed in finite element modeling.

### 1. Series One

A total of eight plain concrete beams are studied in this series, which are designed with five different sizes to investigate the effect of size and concrete compressive strength on the ultimate torsional moment and also the behavior at failure, these two variables are the most important parameters of the plain concrete. All specimens have the same length, the overall length is 3100mm and the length of the beams subjected to torsion is 2390 mm. There is no reinforcement in these beams at all Table (4-2) and Figs [(4-2) and (4-3)] show all details of beams geometry and ANSYS modeling.

**Table (4-2): Details of Specimens (Series 1) [7]**

Specimen	fc' (MPa)	Splitting tensile strength (MPa)	Modulus of rupture (MPa)	Dimensions b×h×L (mm)
S1-PN1	27.56	3.25	4.20	250x250x3100
S1-PN3	28.11	3.29	4.24	250x380x3100
S1-PN4	29.14	3.35	4.32	250x500x3100
S1-PN6	20.00	2.77	3.58	250x500x3100

S1-PN7	25.00	3.10	4.00	250x500x3100
S1-PN8	35.00	3.67	4.73	250x500x3100
S1-PN9	27.01	3.22	4.16	150x280x3100
S1-PN11	30.80	3.44	4.44	150x500x3100

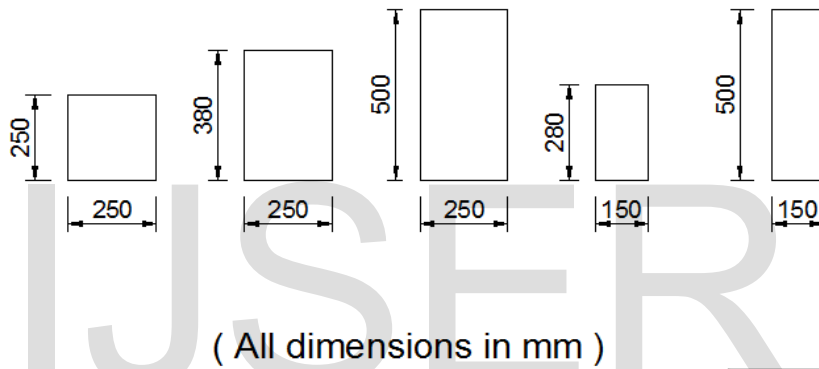
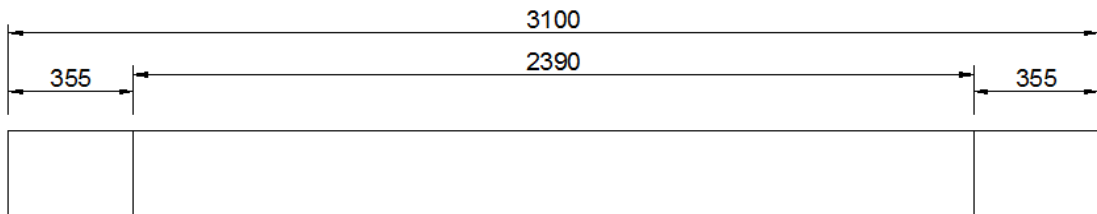


Figure (4-2): Beams specimen geometry (Series 1) [7]

## 2. Series Two

In this series, the study is carried out on plain high strength concrete beams based on the experimental study by Bakhsh et. al. [80]. The loading condition is the same for all these groups, the length of the specimens which are considered as plain concrete is 740 mm while the ends are reinforced , the width is enlarged at these ends by 40 mm to reduce stress concentration. All details of specimens geometry are illustrated in the Table (4-3) and shown by Figs [(4-4) and (4-5)].

Table (4-3): Details of specimens (Series 2) [80]

Specimen	fc' (MPa)	Splitting tensile strength (MPa)	Modulus of rupture (MPa)	Dimensions b×h×L(mm)
S2-PH1	39.39	3.89	5.02	125x250x2180
S2-PH5	59.14	4.77	6.15	=
S2-PH8	68.20	5.12	6.61	=
S2-PH9	68.20	5.12	6.61	188x375x2180
S2-PH10	68.20	5.12	6.61	250x500x2180
S2-PH11	71.43	5.24	6.76	125x250x2180
S2-PH15	89.60	5.87	7.57	=

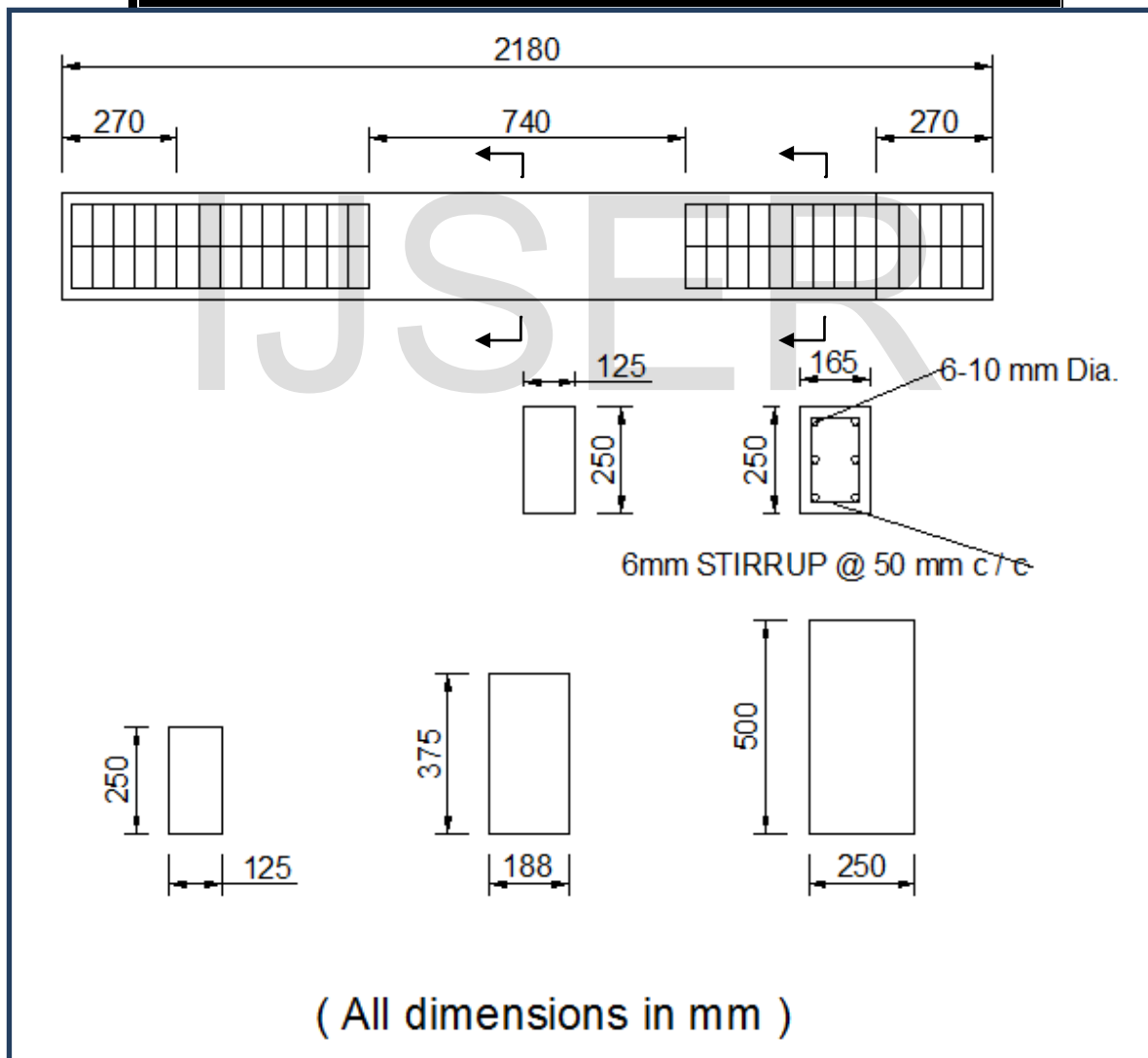


Figure (4-4): Beams specimen geometry (Series 2) [80]



In this series, the same two parameters are investigated as in the previous series which include the concrete strength (high strength) in this series, by changing concrete compressive strength from 39.39 to 89.60 MPa and the second parameter is the size of the beams.

## 6. Presentation and Discussion of Results

### 6.1 Series One

#### 1. Torques at Failure

The experimental and analytical results of the failure torque in addition to the values predicted based on elastic, plastic and skew bending equations are shown in Table (4-6). The ultimate torque of the modeled beams were indicated by the state that the beams no longer can support additional torque (couple) as indicated by the convergence failure of ANSYS program in failing to find a solution. It can be noticed that there is acceptable agreement between results of the present models and the experimental models. A comparison between the ultimate torques of the experimental and ANSYS results is presented. The ratio of the predicted ANSYS ultimate torques to experimental torques ranged from 91.9% to 95.5%. The finite element failure torque underestimates the experimental results, this difference in results can be attributed to the tensile strength of the concrete which is larger than the calculated  $f_t$ .

It can be noticed that, at the first stages, both the experimental and ANSYS models have nearly similar behavior.

By observing the results of the specimens, it is noticed that, by increasing the compressive strength of concrete from 20 to 35 MPa, the value of the ultimate torque increases by 31.9% for specimens with the large section size as shown in Fig. (4-10).

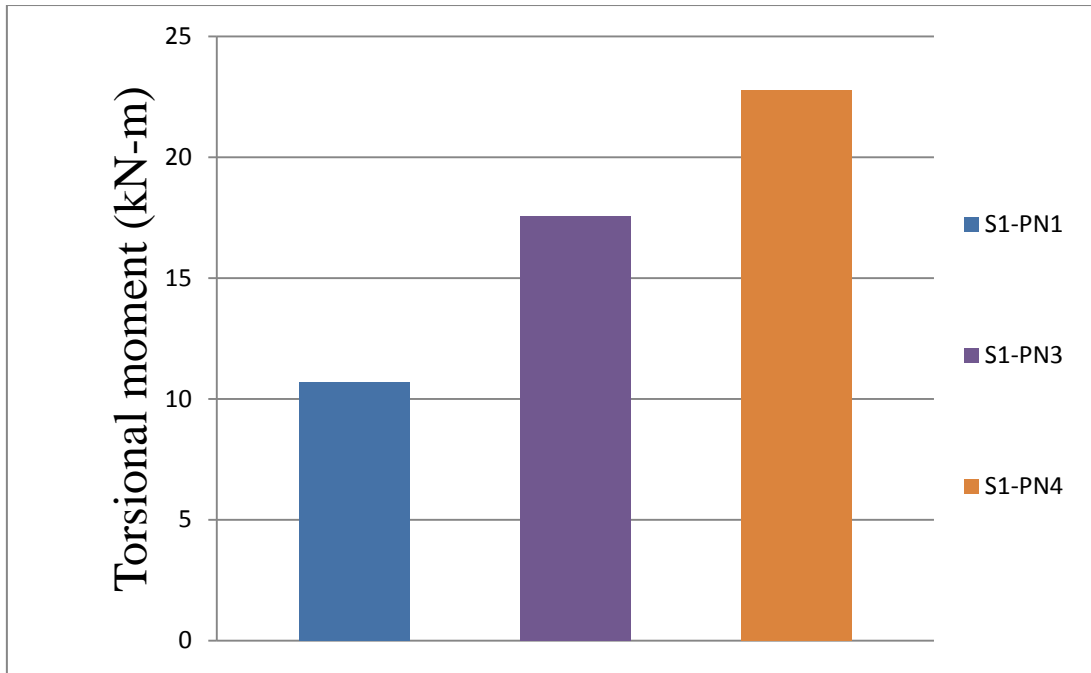
**Table (4-6): Theoretical and experimental results (Series 1)**

Specimen No.	Exp.	Theoretical torsional moment (kN-m)				T (FEM)/ T(Exp.)
		FEM	Elastic	Plastic	Skew Bending	
S1-PN1	11.52	10.69	7.17	11.48	14.76	0.927
S1-PN3	19.09	17.54	12.19	20.64	22.67	0.919
S1-PN4	24.40	22.76	17.78	30.23	30.97	0.933
S1-PN6	-	19.12	14.73	25.04	25.66	-
S1-PN7	-	21.36	16.47	28.00	28.69	-
S1-PN8	-	25.22	19.48	33.13	33.94	-
S1-PN9	6.10	5.64	3.31	5.65	5.89	0.924
S1-PN11	11.41	10.90	7.11	11.80	11.24	0.955



**Figure (4-10): The effect of concrete compressive strength**

Section size and section dimensions are an important factor that affects the ultimate torque for the plain concrete beams, it is noticed that, increasing the depth of the beam from 250 mm to 510 mm can lead to an increase in the torsional strength by 112.9% for the specimen with 250 mm width. For the beams with 150 mm width the torsional strength increases 93.3% as the depth increase from 280 mm to 500 mm as shown in Fig. (4-11).



(a) Specimens with 250 mm width



(b) Specimens with 150 mm width

Figure (4-11): The effect of section size

The elastic theory equation gives lower values of the torque capacities for beams in this series, with the ratio of the elastic torque capacity to experimental torques ranging from 54.3% to 72.8%.

Generally, the torsional moment calculated using the elastic theory equation is a function of the compressive strength of concrete and the section size of the beams, this is also true for the plastic

and skew bending theories , it is obvious that the section size has a significant effect on the torsional moment.

The plastic theory shows good agreement with the experimental torsional capacity compared to the other theories, noting that the section size has a great effect ,this effect is clearly obvious in the large section 250 \* 500 mm as it overestimated the ultimate torsional moment by 23.8%, for the other sizes the variation is below 15% of the experimental torsional capacity.

The skew bending theory gives a slightly larger torsional capacity than the plastic theory, the ratio of the skew bending ultimate torques to experimental torques ranges from 96.6% to 132.6%.

### 3. Torque-Twist Plots

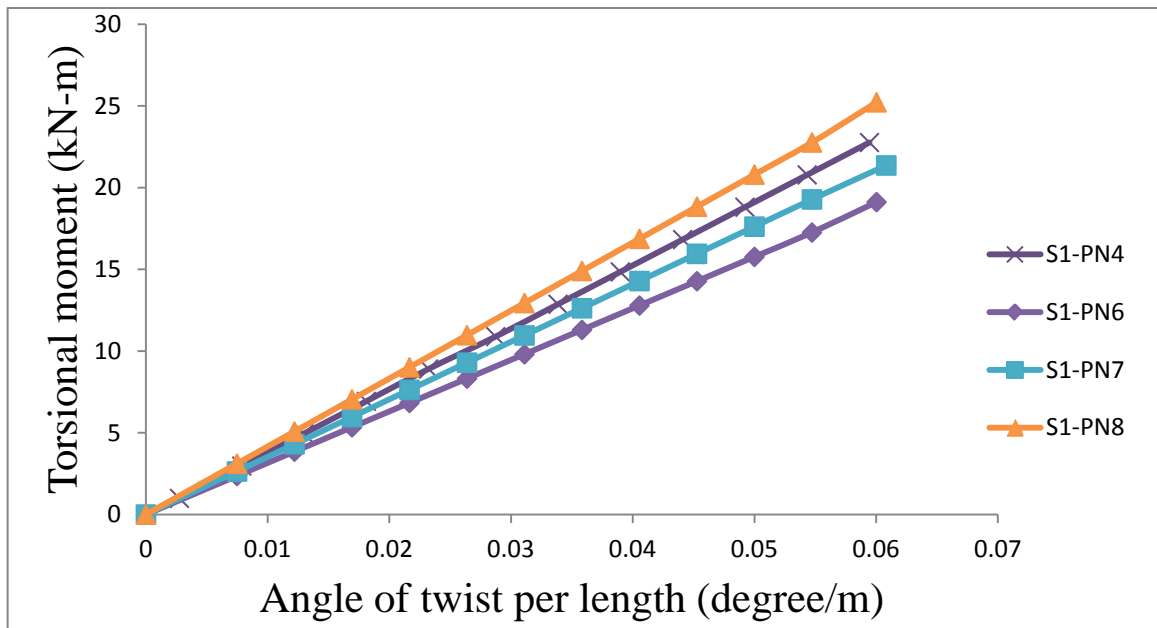
Table (4-7) contains all the details of twist results. For ANSYS, the ultimate twist angles are calculated, by measuring the displacements of specified points at the ends of the specimen and then calculating the twist angle at same location for the experimental beams.

**Table (4-7): Theoretical and experimental twist at ultimate torque**

(Series 1)

Specimen	Angle of twist per length (DEGREE/m) (Exp.)	Angle of twist per length (DEGREE/m) (FEM)	Twist (FEM) / Twist (Exp.)
S1-PN1	0.111	0.071	0.64
S1-PN3	0.099	0.059	0.59
S1-PN4	0.077	0.059	0.77
S1-PN6	-	0.060	-
S1-PN7	-	0.060	-
S1-PN8	-	0.060	-
S1-PN9	0.187	0.123	0.65
S1-PN11	0.167	0.119	0.71

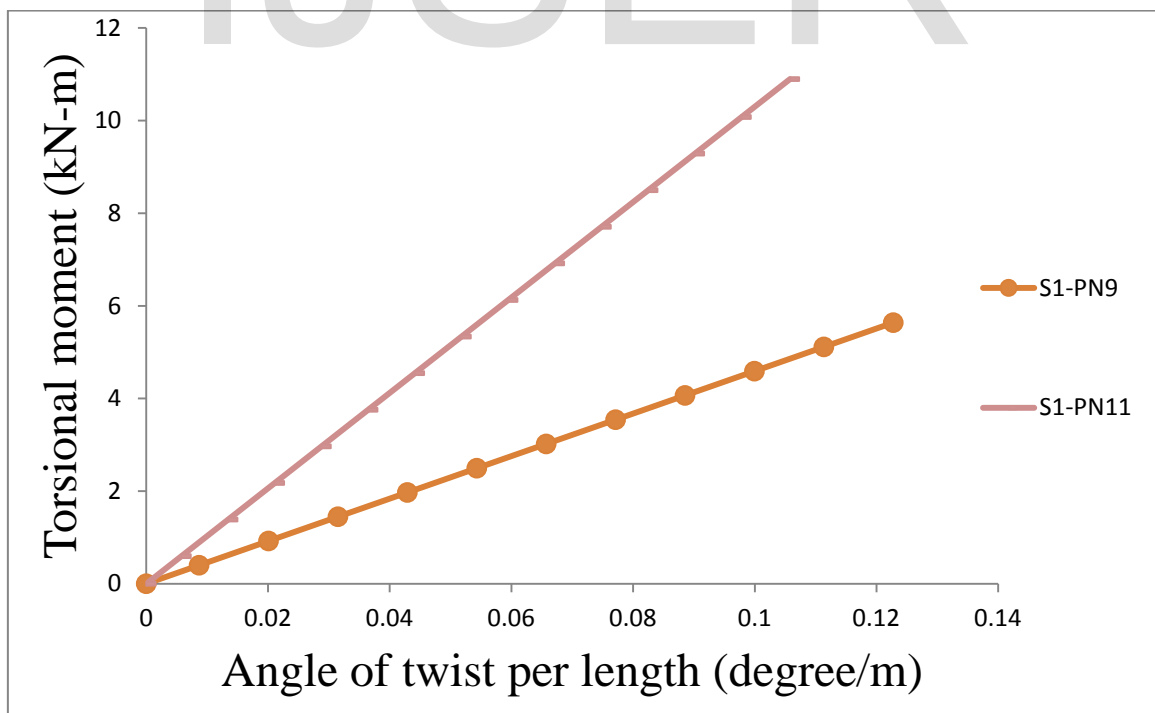
A slight increase in the twist angle at the ultimate torque is observed as a result of increase the compressive strength of concrete, it is not clearly obvious in the large size beams ,but it can be noticed in the small size beams as shown in Fig. (4-13) .



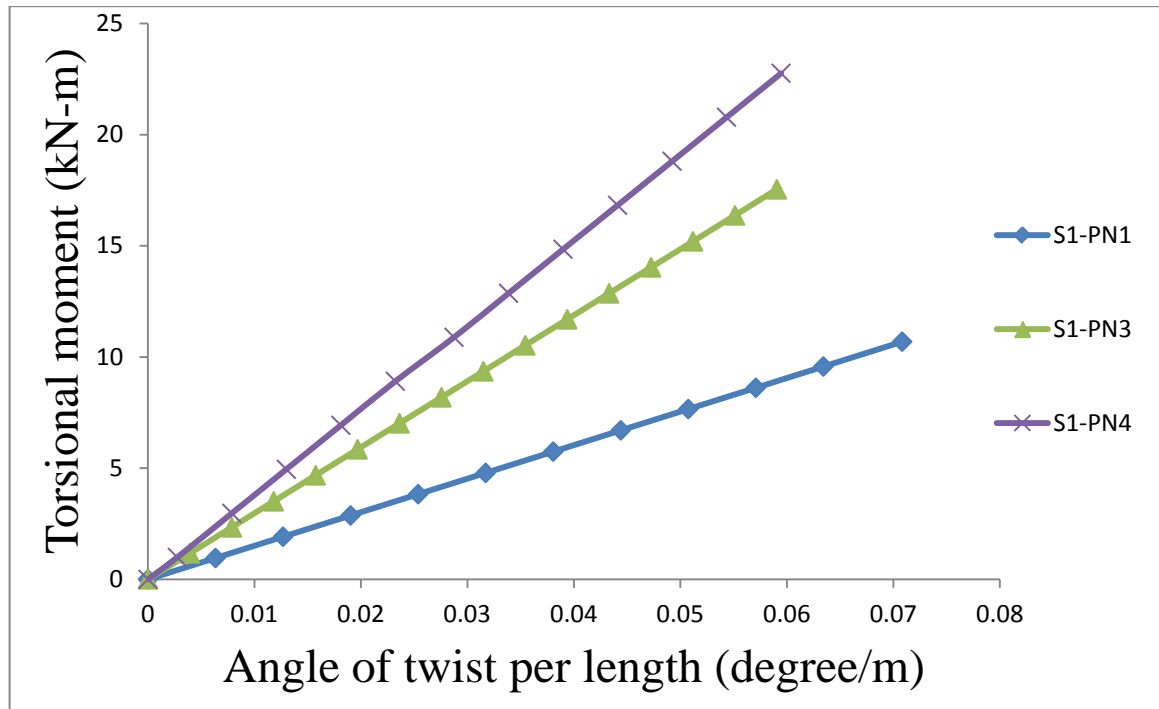
(a) Specimens with large size section (contd ...)

Figure (4-13): Effect of compressive strength on twist

Also, the results by ANSYS show that a small decrease in the angle of twist as the section size increases for the cases of (150 mm and 250 mm width) as shown in Fig. (4-14)



(a) Specimens with 150 mm width (contd ...)



(b) Specimens with 250 mm width

Figure (4-14): Effect of section size on the angle of twist

#### 4.4.2 Series Two

##### 1. Torques at Failure

All the results for the failure torque from the experimental and analytical models and the values predicted from elastic, plastic and skew bending theories are listed in Table (4-8). It can be noticed that there is acceptable agreement between results of the analytical models and the experimental tests.

A comparison between the ultimate torques of the experimental and FEM results is presented. The ratios ranged from 85% to 99 % of the predicted ANSYS ultimate torques to experimental work torques. The finite element failure torque underestimates the experimental results by about 15 % maximum difference. This difference in results can be attributed to the same reasons as in series one, also it can be noticed that for the experimental results the same

concrete strengths may give different torsional capacities, but in the FEM models, results show that each grade of concrete strength results in unique value of torsional capacity.

Both the experimental and ANSYS models have nearly similar behavior at the first stages for all specimens.

**Table (4-8): Theoretical and experimental results (Series 2)**

Specimen No.	Exp.	Theoretical torsional moment (kN-m)				T (FEM)/ T(Exp.)
		FEM	Elastic	Plastic	Skew Bending	
S2-PH1	4.44	4.22	2.53	4.29	4.41	0.95
S2-PH5	5.81	5.26	3.10	5.26	5.41	0.91
S2-PH8	7.10	6.10	3.33	5.65	5.81	0.86
S2-PH9	-	17.43	11.31	19.14	19.70	-
S2-PH10	-	28.07	26.66	45.16	46.45	-
S2-PH11	7.32	6.30	3.41	5.78	5.94	0.86
S2-PH15	8.07	7.48	3.82	6.47	6.66	0.93

The results of the specimens investigated in this series showed that, the ultimate torque is directly proportional with the concrete compressive strength, by increasing the compressive strength of concrete from 39.39 to 89.00 MPa, the value of the ultimate torque increases by 77.25% for specimens having the same section size as shown in Fig. (4-15).

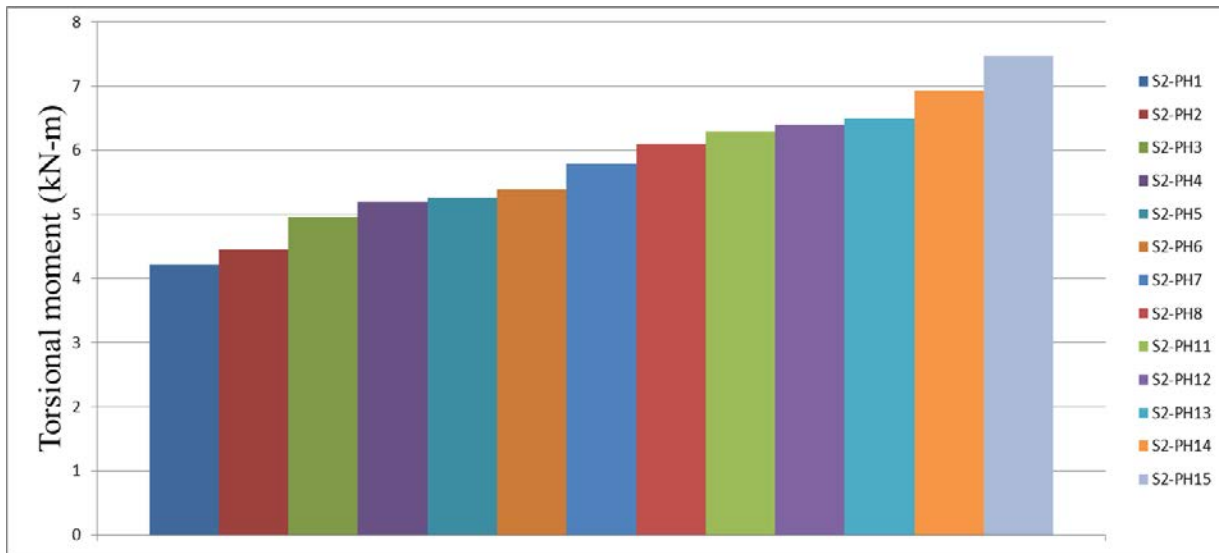


**Figure (4-15): The effect of concrete compressive strength**

The large increment can be obtained by increasing the section size, changing section dimensions of the specimen S2-PH8 from 150 mm \* 250 mm to 250 mm \* 500 mm, it leads to an increase in the torsional strength of 460% as shown in Fig. (4-16).

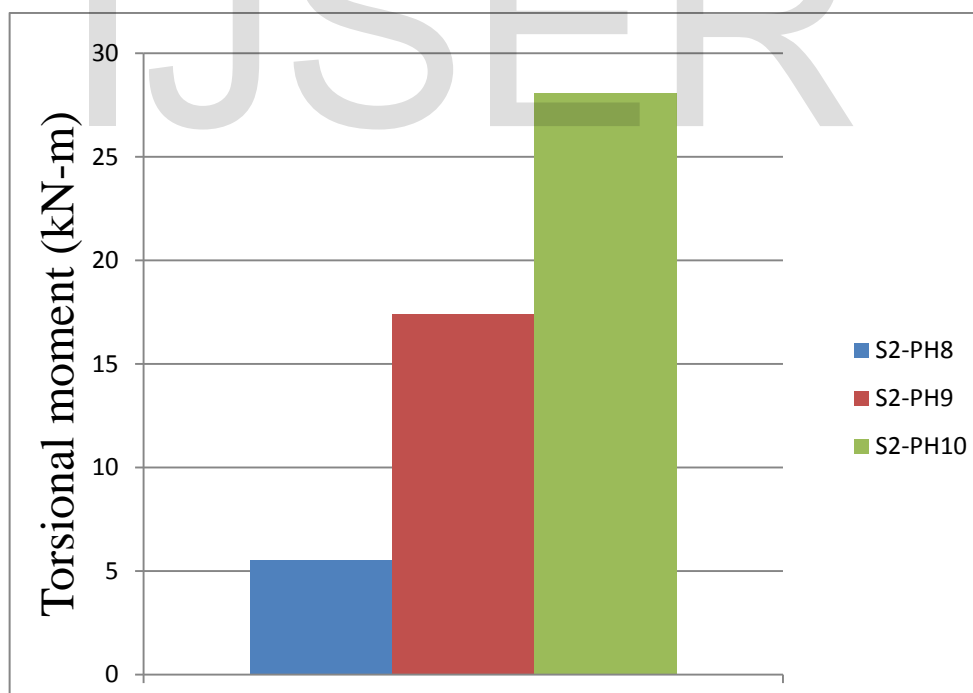


**Figure (4-16): The effect of section size**

The first theory which is the elastic theory underestimates the torque capacities for beams in this series, the ratio of the elastic ultimate torques to FEM ultimate torques vary from 51% to 60% except for specimen S2-PH9 and S2-PH10, which have ratios equal to 64.8% and 94.9%



The best agreement is achieved from plastic theory which shows good ratios with the FEM torsional capacity compared to the other theories equation, this agreement ranges from 86.4% to 102.0% as shown in Fig. (4-17), except for the large and medium specimen that shows differences equal to 9.8% for the medium size specimen and 60.8% for the large size specimen,

The skew bending theory gives a slightly larger torsional capacity than the plastic theory, and also shows good agreement with the theoretical results as shown in Fig. (4-17), the ratio of the skew bending ultimate torques to FEM model torques ranged from 88.9% to 165.4%.

## 2. Torque-Twist Plots

All the details of twisting angle results are listed in table (4-9). The ratios between FEM and experimental angle of twist vary from 0.45 to 0.58.

**Table (4-9): Theoretical and experimental twist at ultimate torque**

**(Series 2)**

Specimen	Angle of twist per length (DEGREE/m) (Exp.)	Angle of twist per length (DEGREE/m) (FEM)	Twist (FEM) / Twist (Exp.)
S1-PH1	0.28	0.16	0.56
S2-PH5	0.35	0.18	0.51
S2-PH8	0.38	0.19	0.50
S2-PH9	-	0.41	-
S2-PH10	-	0.51	-
S2-PH11	0.39	0.19	0.49
S2-PH15	0.40	0.21	0.53

A slight increase in the twist angle at the ultimate torque is noted as a result of increase the compressive strength of concrete, in Fig. (4-19) only four specimen out of thirteen are plotted to clarify the compressive strength effect on the twist, an increment equal to 31.5 % in the angle of twist is evident as the compressive strength of concrete increases from 39.39 MPa to 89 MPa.

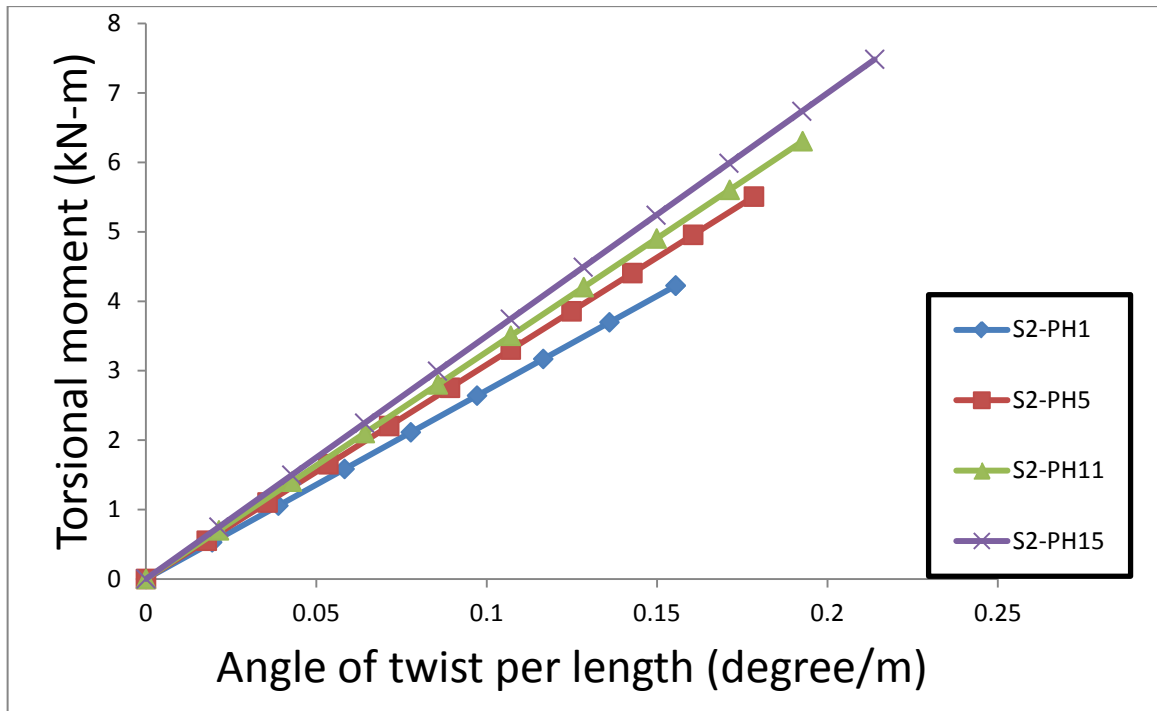


**Figure (4-19): Effect of compressive strength on twist**

Also, the results by ANSYS show that there is an increase in the twisting angle for larger sections as shown in Fig. (4-20), the increment is large for the medium specimen referred to the specimen S2-PH8

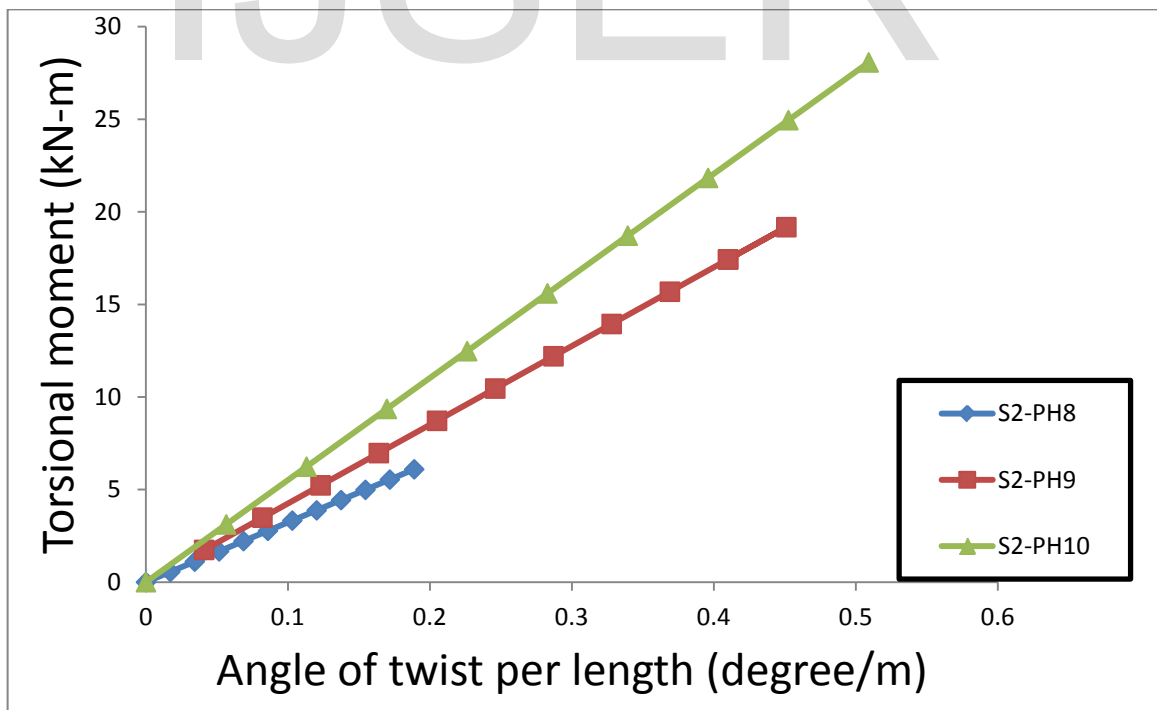


**Figure (4-20): Effect of section size on the angle of twist**

## 5-1 Conclusions

- 1) The nonlinear FE model, which was adopted in the current study, is appropriate for simulation of the behavior of plain concrete beams subjected to torsion and capable of predicting the ultimate torque, ultimate angle of twist for the beams and the overall behavior with good accuracy.
- 2) The size of the beams is found to be the most important parameter that affects ultimate torque in the plain concrete beams, where the torsional capacity increases in direct proportion to section size, and the percentage of increase reaches (112.9 and 460%) for **NSC** and **HSC** beams respectively.
- 3) The failure in the plain concrete beams is sudden so that the crack pattern cannot be predicted by ANSYS.
- 4) The plastic theory is the best to estimate the ultimate, torsional, strength of beams with plain concrete, but does not take the size effect adequately into account especially for large beams.

IJSER